

A new integrated method to design of rock structures

Okay C. Aksoy^{*1}, Gulsev G. Uyar^{2a}, Semih Utku^{3a}, Suleyman Safak^{1a} and Vehbi Ozacar^{1a}

¹Dokuz Eylul University, Engineering Faculty, Department of Mining Engineering, Izmir-Turkey

²Hacettepe University, Engineering Faculty, Department of Mining Engineering, Ankara-Turkey

³Dokuz Eylul University, Engineering Faculty, Department of Computer Science, Izmir-Turkey

(Received February 26, 2019, Revised June 13, 2019, Accepted June 14, 2019)

Abstract. Rockmass parameters are used in the design of engineering structures built in rock and soil. One of the most important of these parameters is the rockmass E_{mass} (E_{mass}). Determination of the E_{mass} of rockmass is a long, hard and expensive job. Therefore, empirical formulas developed by different researchers are used. These formulas use the elastic modulus of the material as a parameter. This value is a constant value in the design. However, engineering structures remain under different loads depending on many factors, such as topography, geometry of the structure, rock / soil properties. Time is other important parameter for rock/soil structure. With the start of the excavation, the loads that the structure is exposed to will change and remain constant at one level. In the new proposed method, the use of different E_{mass} calculated from empirical formulas using the different material elastic modulus, which has different values under different loads as time dependent, was investigated in rock/soil structures during design. The performance of the stability analysis using different deformation modules was questioned by numerical modeling method. For this query, a sub-routine which can be integrated into the numerical modeling software has been developed. The integrated sub-routine contains the formula for the E_{mass} , which is calculated from the material elasticity modules under time dependent and different constant loads in the laboratory. As a result of investigations conducted in 12 different field studies, the new proposed method is very sensitive.

Keywords: rock mechanics, numerical modeling, time-dependent deformation, stability analysis

1. Introduction

Numerical modeling methods used in rock engineering are studied in detail by Jing and Hudson (2002). In rock engineering project, final design processes are time consuming, expensive and need great experience. Feng and Hudson (2010) explained what should have been done to find out how much information is needed in a particular project. Feng and Hudson (2004) discussed the ways ahead for rock engineering design methodologies and presented two updated flow charts which is given in Fig. 1.

Information, design geometry and uncertainties about applications in a design are present in the literature (Mazzoccola *et al.* 1997, Anderson *et al.* 2004, Feng and An, 2004; Hudson and Feng 2007).

In the beginning of a design process, definition and characterization of the rock mass must be introduced. In literature, a number of rock mass classification systems have been defined (Table 1).

Rock mass classification methods are extensively used in preliminary phase of the design. Rock mass properties (e.g. deformation modulus of rock mass- E_{mass}) needed in a design process are determined by empirical equations based on the system relevant. The static E_{mass} is among the parameters that represents the mechanical behaviour of the

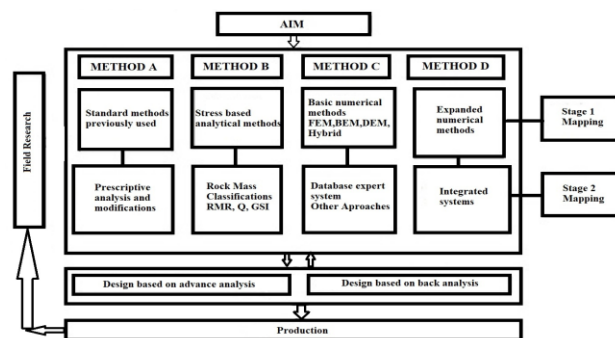


Fig. 1 Updated flowchart for rock mechanics modeling (prepared from Feng and Hudson 2004)

rock and the rock mass. As well known, insitu deformation tests are quite expensive and difficult to carry out (Aksoy *et al.* 2012, Palmstrom and Singh 2001). They are mostly conducted in special test adits or drifts excavated by conventional drill and blast techniques, in an opening with a span of 2 m and a height of 2.5 m, using various forms of testing methods. It is well known that in-situ tests conducted to measure E_{mass} of the rock mass are subjected to measurement errors induced from the equipment, test site preparation and blasting damage in the test adit (Palmstrom and Singh 2001). Also, such measurements are carried out in a limited volume of the rock mass. Therefore, good site characterizations of the rock mass and use of the appropriate indirect method may in many cases yield better results than that of expensive in-situ measurements (Palmstrom and Singh 2001). Some empirical equations for

*Corresponding author, Ph.D.

E-mail: okay.aksoy@deu.edu.tr

^aPh.D.

the determination of E_{mass} are given in Table 2. These equations are used to calculate the $d E_{mass}$ with different geotechnical conditions. As seen in Table 2, empirical equations use the material elastic modulus (E_i) as a parameter for calculating the E_{mass} . This parameter is a constant value, which obtained from the laboratory and is calculated from the point corresponding to 50% of the deformation test curve. However, it is very difficult to detect the loads which the rock mass faced in nature. The rock/soil structure which is designed has been faced different loads depending on topographical conditions, geometry of engineering structure, groundwater, depth etc. The rock/soil structure can be exposed different loads which is different from the load 50% (which obtained from the deformation test and used in design phases). In this case, it is a requirement for the design to be more accurate to use a different and time-dependent E_i for the different loads to which the rock material (hence rock/soil mass) is exposed. E_i , which is used to estimate the E_{mass} of rock mass is included as a parameter in the formulas as displayed in Table 2. This value is a static value and does not vary with time. Figure 2 exhibits the E_i values obtained from the deformability test results. E_i value which is the slope of stress-strain curve at 50% of the ultimate load and the poisson ratio (horizontal/vertical deformation) are used as parameters. The static E_i is used to estimate the rock mass E_{mass} , which is one of the most important parameters in numerical analyses.

The most important question to ask will be; whether or not the stability of the rock structure will be risky if the amount of stress to which the rock structure will be subjected to is just above the value set for the E_i ? Or, on the contrary, whether or not it will be a production overdesign if the amount of stress to which rock mass is subjected to is lower than the amount of stress used to estimate the E_i ? This new integrated proposed is thought to have different values for some parameters under different loads and the algorithm is developed based on this idea. The stages of the new proposed integrated method are given in Figure 3.

Twelve different fields have been selected for this study, which will bring a different rockmass perspective to numerical modeling studies. In the result of the geotechnical studies carried out in such fields, rock mass characterizations of each field were determined separately. Laboratory studies and software studies have been carried out to develop the new integrated method. Numerical analyses were performed to confirm the results of the research. Results of numerical studies and in-situ measurements carried out in sites were compared.

2. Theoretical Basis of New Integrated Method

Rock mass classification systems and formulas used to obtain rock mass E_{mass} are displayed in Table 1 and Table 2. The E_{mass} , obtained from the formulas are widely used in numerical analyses. In rock excavation, the load on the rock structure gradually increases and remains constant at a certain level. Then, the load on the rock structure will change upon new excavation stage and will become stable again. Such dynamic cycle will continue following new

Table 1 Some rock mass classification and characterization systems (revised from Palmstrom 1995, Edelbro *et al.* 2006, Palmstrom and Stille 2007)

Name	Form and type(*)	Main applications and remarks	Author and first revision
Terzaghi rock load classification system	Descriptive and behaviouristic form Functional type	Tunnels with steel support	Terzaghi (1946)
Lauffer's Stand-up time classification	Descriptive form General type	For input in tunnelling design	Lauffer (1958)
New Australian Tunneling Method (NATM)	Descriptive and behaviouristic form Tunneling concept	For excavation and design in incompetent ground	Rabcewicz (1964, 1965)
Rock classification for rock mechanical purposes	Descriptive form General type	For input in rock mechanics	Patching and Coates (1968)
Unified classification of soils and rocks	Descriptive form General type	Based on particles and blocks for communication	Deere <i>et al.</i> (1969) in Deere and Deere (1988)
Rock Quality Designation (RQD)	Numerical form General type	Based on core logging; used in other classification systems	Deere <i>et al.</i> (1967)
Size-strength classification	Numerical form Functional type	Based on rock strength and block diameter,	Franklin (1975)
Rock Structure Rating (RSR)	Numerical form Functional type	For design of (steel) support in tunnels	Wickham <i>et al.</i> (1972)
Rock Mass Rating (RMR)	Numerical form Functional type	For design of tunnels, mines, and foundations	Bieniawski (1973)
Q Classification System	Numerical form Functional type	For design of support in underground excavation	Barton <i>et al.</i> (1974)
Mining RMR (MRMR)	Numerical form Functional type	Rock support in mining	Laubscher (1975) in Laubscher (1977)
Typological classification	Descriptive form General type	For use in communication	Matula and Holzer (1978)
Unified rock classification system	Descriptive form General type	For use in communication	Williamson (1980)
Basic geotechnical classification (BGD)	Descriptive form General type	For general applications	ISRM (1981)
Slope Mass Rating (SMR)	Numerical form Functional type	Forecast stability problems and support techniques	Romano (1985)
Geological Strength Index (GSI)	Numerical form Functional type	Indicates the strength of rock masses,	Hoek (1994)
Rock Mass Index (RMi)	Numerical form Functional type	Rock engineering, general characterization, design of support	Palmstrom (1995)

excavation stages. Deformation of rock material will vary owing to the changes in rock load in each dynamic cycle (depending on the time) and will remain constant afterwards. In this case, it is expected that E_{mass} of the rock mass will change under constant load owing to the changes in E_i and Poisson Ratio's depending on time. Hence, the results will differ by the changes in E_{mass} and Poisson's Ratio in numerical modeling. E_{mass} value is calculated based

Table 2 Empirical equations for the determination of E_{mass}

Researchers	Equation	Notes
Bieniawski (1973)	$E_{mass} = 2 RMR - 100$ (GPa)	for $RMR > 50$
Serafim and Pereira (1983)	$E_{mass} = 10^{(RMR-10)/40}$ (GPa)	for $RMR < 50$
Nicholson and Bieniawski (1990)	$E_{mass} = \frac{E_i}{100} \left[0.0028 RMR^2 + 0.9 \exp\left(\frac{RMR}{22.82}\right) \right]$	
Mitri <i>et al.</i> (1994)	$E_{mass} = E_i \left[0.5 \left\{ 1 - \cos\left(\pi \frac{RMR}{100}\right) \right\} \right]$	
Palmstrom (1996)	$E_{mass} = 5.6 RMi^{0.375}$ (GPa)	for $1 > RMi > 0.1$,
Palmstrom and Sing (2001)	$E_{mass} = 7 RMi^{0.4}$ (GPa)	for $1 > RMi > 30$,
Hoek and Brown (1997)	$E_{mass} = \sqrt{\frac{\sigma_{ci}}{100}} 10^{\frac{(GSI-10)}{40}}$ (GPa)	for $\sigma_{ci} < 100 MPa$
Read <i>et al.</i> (1999)	$E_{mass} = 0.1 \left(\frac{RMR}{10}\right)^3$ (GPa)	
Barton (2002)	$E_{mass} = 10 Q_c^{\frac{1}{3}}$ $Q_c = Q \sigma_{ci} / 100$	
Kayabasi <i>et al.</i> (2003)	$E_{mass} = 0.135 \left[\frac{E_i (1 + RQD/100)}{WD} \right]^{1.1811}$	
Gokceoglu <i>et al.</i> (2003)	$E_{mass} = 0.001 \left[\frac{(E_i / \sigma_{ci})(1 + RQD/100)}{WD} \right]^{1.5528}$	
Sonmez <i>et al.</i> (2004)	$E_{mass} = E_i (s^a)^{0.4}$ $s = \exp\left[\frac{(RMR - 100)}{9}\right]$ $a = 0.5 + 1/6 \left[\exp(-GSI/15) - \exp(-20/3) \right]$	
Sonmez <i>et al.</i> (2006)	$E_{mass} = E_i 10^{\left[\frac{(RMR-100)(100-RMR)}{4000} \exp(-RMR/100)\right]}$	
Hoek and Diederichs (2006)	$E_{mass} = E_i \left(0.02 + \frac{1-D/2}{1 + e^{(60+15D-GSI)/11}} \right)$	no deformation measurement $E_i = MR \cdot \sigma_{ci}$

RQD: rock quality designation, RMR: rock mass rating, RMi: rock mass index, Q: rock mass quality rating, GSI: geological strength index, σ_{ci} : UCS of intact rock, E_i : E_{mass} of intact rock, E_{mass} : E_{mass} of rock mass, MR: modulus ratio, WD: weathering degree, D: disturbance factor, s, a: Hoek-Brown rock mass constants

on the experimental E_i value, as a function of time and load. Hence, the new approach can be suggested for the numerical models which are based on time-dependent data obtained under various constant loads. This new approach was integrated in a new software as time-load-dependent formula. On the other hand, there are many valuable research about new methods and new applications with

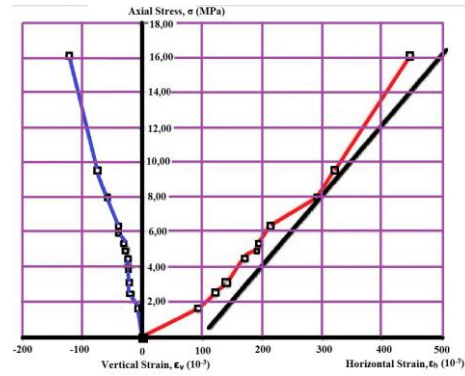


Fig. 2 The result of deformability test

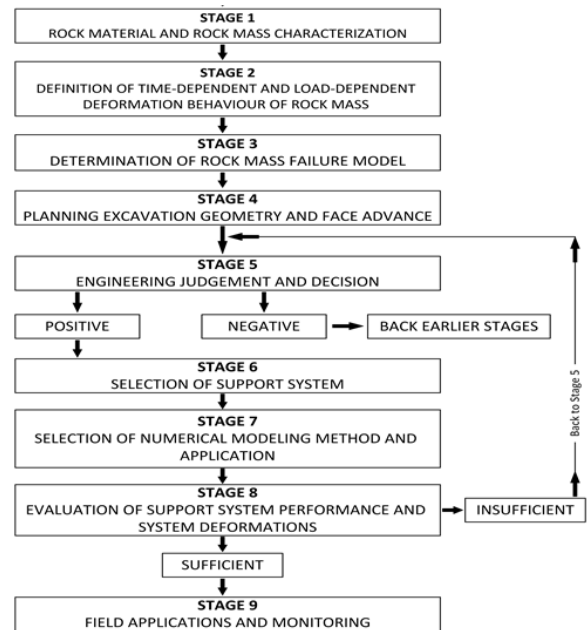


Fig. 3 Stages of the new proposed integrated method



Fig. 4 Servo-controlled compressive loading press for time-dependency experiments

laboratory and field works in the literature about rocks deformation behavior and characterization (Aksoy *et al.* 2016, Gu 2015, Jiang *et al.* 2018, Taravani and Ardakani 2018, Rooh *et al.* 2018, Zhang *et al.* 2018, Palchik 2018).

2.1 Laboratory research

Routine rock mechanics laboratory experiments were

Table 3 Types, properties and lithology of rocks tested

Sample No.	Rock Properties	Lithology and Rock Description	Rocks
ACong 1 (Ankara-Afyon HRST Construction)	UCS _i :9.90 MPa, E _i : 1180 MPa, ν: 0.26, Φ _i :42.11° c _i :0.173 MPa	Gray-ligth gray, wavy structure, weak-very weak, often clay band, Conglomera, GSI: 30	
ACong 2 (Ankara-Afyon HRST Construction)	UCS _i : 28.43 MPa E _i : 2050 MPa ν: 0.27, Φ _i :44.22° c _i : 0.191 MPa	Gray-ligth gray, wavy structure, hard-medium, often clay band, Conglomera, GSI: 40	
EM (Soma-Eynez Underground Coal Mine)	UCS _i : 24.29 MPa E _i : 1910 MPa ν: 0.23, Φ _i :45.36 c _i :0.322 MPa	Homegeneous, hard, massive structure. Fresh surfaces are Ligth gray-green, They are medium thick layers. Marl, GSI: 50	
TC (Tavsanlı-Ömerler Underground Coal Mine)	UCS _i : 28.40 MPa E _i : 3210 MPa ν: 0.33, Φ _i :39.92 c _i :0.297 MPa	Gray-dark gray, generally jointed, hard-medium strength, Claystone, GSI: 45	
IC (Soma-Işıklar Underground Coal Mine)	UCS _i : 20.74 MPa E _i : 4900 MPa ν: 0.31, Φ _i : 38.94 c _i : 0.793 MPa	Gray-dark gray, locally jointed, generally massive, hard-medium-weak strength, Claystone, GSI: 50	
IL (Soma-Işıklar Underground Coal Mine)	UCS _i : 52.07 MPa E _i : 4420 MPa ν: 0.27, Φ _i : 53 c _i : 0.862 MPa	Gray-ligth gray, generally massive, locally jointed, clay infilling, hard, sometimes medium, Limestone, GSI: 60	
ICong (Soma-Işıklar Underground Coal Mine)	UCS _i : 12.39 MPa E _i : 8360 MPa ν: 0.37, Φ _i : 42.04 c _i : 0.167 MPa	Gray-dark gray, generally jointed, medium-weak strength, generally massive, jointed with clay infilling Conglomera, GSI: 40	
IM (Soma-Işıklar Underground Coal Mine)	UCS _i : 29.42 MPa E _i : 1560 MPa ν: 0.26 Φ _i : 47.70 c _i : 0.445 MPa	Homogeneous structure, hard and generally massive. Gray-ligth gray, and when they are broken, they turn into a light gray color called ash color. They are medium thick layers., Marl, GSI: 55	
MM (Ordu-Mesudiye RTConstruction)	UCS _i : 62.07 MPa E _i : 1740 MPa ν: 0.30 Φ _i : 46.00 c _i : 1.048 MPa	Dark gray-gray, generally massive, locally jointed, hard-medium, Marl, GSI: 65	
PS (Soma-Kınık Underground Coal Mine)	UCS _i : 20.16 MPa E _i : 1210 MPa ν: 0.29, Φ _i : 45.86 c _i : 0.258 MPa	Gray – Ligth gray, often–very often jointed schistosity planes slippery shiny, disintegrated partially, weak-very weak, Schist, GSI: 45	
TS-1 (Tokat-Topçam RTConstruction)	UCS _i : 52.26 MPa E _i : 4440 MPa ν: 0.31, Φ _i : 60.27 c _i : 0.923 MPa	Gray-dark gray, massive-jointed with clay band, generally hard-medium strength Siderite, GSI: 65	
TS-2 (Tokat-Topçam RTConstruction)	UCS _i : 80.63 MPa E _i : 12020 MPa ν: 0.23, Φ _i : 62.41 c _i : 1.247 MPa	Gray-ligth gray, hard-very hard, generally massive, Siderite, GSI: 75	

HRST: High Speed Railway Tunnel; RT: Railway Tunnel

primarily performed to determine the significant parameters; E_i and Poisson Ratio of the rock material. Such parameters will define the elasticity of the rock mass via E_{mass} in numerical analyses. This definition represents how the rockmass will display a deformation behavior against the load in the model. As described above, E_i is a parameter in the formulas used to determine the E_{mass} of the rock

mass (E_{mass}). In the formulas, E_{mass} will vary as E_i changes. As known, E_i and Poisson Ratio of the rock material can vary under constant load over the time. A servo-controlled compressive loading machine was used to measure the changes in rock material properties in the laboratory (Figure 4).

The deformation which develops under constant load is

Table 4 Geotechnical properties of the rocks studied

Sample	E_i (from Laboratory Tests) (Mpa)	RMR	Q	GSI	σ_i (from Laboratory Tests) (Mpa)
Afyon Conglomerate- 1	1180	33	0.46	30	9.99
Afyon Conglomerate- 2	2050	42	0.80	40	13.07
Eynez Marl	1910	54	3.04	50	24.29
Tuncbilek Claystone	3210	49	2.18	45	28.40
Isiklar Marl	1560	59	5.29	55	29.42
Isiklar Conglomerate	8360	48	1.56	40	12.39
Isiklar Claystone	4900	56	3.79	50	20.74
Isiklar Limestone	4420	63	8.26	60	52.07
Mesudiye Marl	1740	71	22.45	65	62.07
Polyak Schist	2090	53	2.72	45	20.16
Topcam Sandstone-1	4440	68	14.39	65	52.26
Topcam Sandstone-2	12020	80	68.19	75	80.63

called creep in the literature (Barla 1995). Such experiments are usually carried out on rock materials such as clay and rock salt. In general, the load will gradually rise depending on the degree of increase in the plastic zone diameter following an excavation in a tunnel and will reach a point at which it will remain constant after this step.

The main goal of this research is to integrate the load development phases into numerical models and to switch from static to dynamic phases. For this purpose, it is aimed at describing the behaviors of the rock material using laboratory equipment with given technical specifications as follows.

The servo-controlled compressive loading press designed to determine the deformation behavior of rock materials can apply homogeneous load on the sample with high strength, 4-column loading bodies, in compliance with the ASTM E139 standards. The 600 kN capacity loading shaft is supported by a mechanical spring system. The equipment which measures the deformation for a long time, uses hydraulic pressure. After reaching the desired load, the submerged tray system can be locked with the mechanical lock with the mechanical spring force to ensure the long-term testing. Load measurement and control are performed between 2% and 100% of the loading capacity. Absolute type position sensor system 5 wireless communicable absolute type sensors, 8 channel data collector, timer function and can detect the change of the deformations on the samples and the measurement capacity can be measured with the accuracy of 12.7 mm and 1 micron. Controlled tests for system load and deformation measurements can be carried out with hydraulic control with DOLI-controlled servo technology. The control unit operates with closed-loop control, i.e. PID control. The electronic control unit of

the system is DOLI EDC 220 mod. A total of 7 sensors can be connected with 2 internal, 2 external and 1 RS 232/485 channel. The control unit can operate at 1000 data sampling rates per second (1kHz / s).

This laboratory equipment was used to examine the variation of the E_i and Poisson's Ratio values with time under constant load applied on intact rock samples taken from 12 different sites. The samples, geotechnical characteristics of working fields and test results of the tests are given in Table 3, 4 and Figure 5, respectively.

The geotechnical differences of the study areas are given in Table 3 and 4. As it is seen here, in this study, a wide geotechnical perspective has been used from very weak rock mass to very strong rock mass. The E_i values obtained by the conventional test method are also illustrated in the same table. According to the test results, under constant load, E_i values were seen to reduce in all samples. Poisson Ratio, which is defined as the ratio of the amount of lateral deformation to the amount of vertical deformation, is the inverse of E_i . Principally, as the applied constant load increases, the ν also increases. On the other hand, under constant load, lateral deformation is seen to occur more than the vertical deformation. Also, the cohesion will play an effective role in time-dependent failures when the samples are under constant load.

The changes in E_i values were examined following the tests in the laboratory. The changes in E_i will directly induce a change in E_{mass} values. In such case, the results in numerical modeling are also expected to change.

Besides, the time-dependent variation in E_i values under constant loads is given in Table 6. The loads applied in the tests are 50%, 60%, 70% and 80% of the UCS_i of the rocks selected.

When Afyon Conglomerate 1 sample is considered as an example, the E_i value determined by the conventional method is 1180 MPa. Different E_i values are encountered on the same sample when E_i is examined for different constant loads and time dependent experiments. When Table 5, which is the summary of the graphs shown in Table 4 is examined the minimum E_i value under 5 kN constant load of Afyon Conglomerate 1 sample is 1540 MPa and the maximum E_i value is 1570 MPa, while the minimum E_i value under constant load of 20 kN is 1690 MPa and the maximum E_i value is 1710 MPa. For different constant loads affecting the same sample, the values of E_i will change with time. In the tests carried out, when examined for this sample, there is a difference of 9.74% between the minimum E_i values and 8.91% between the maximum E_i values. This trend is approximately same for the other samples.

As stated before, one of the easiest ways to estimate the E_{mass} value will be the use of empirical equations. E_{mass} values were obtained from empirical equations developed by various researchers as shown in Table 6. These values are used in numerical modeling under the current methodology and are typed in bold characters. E_{mass} values which are used within the scope of the new methodology are the values given in Table 5 and are produced by using time-dependent E_i values at various constant loads. As can be seen in the Table 6, E_{mass} will take different values for different constant loads depending on the time. This will be

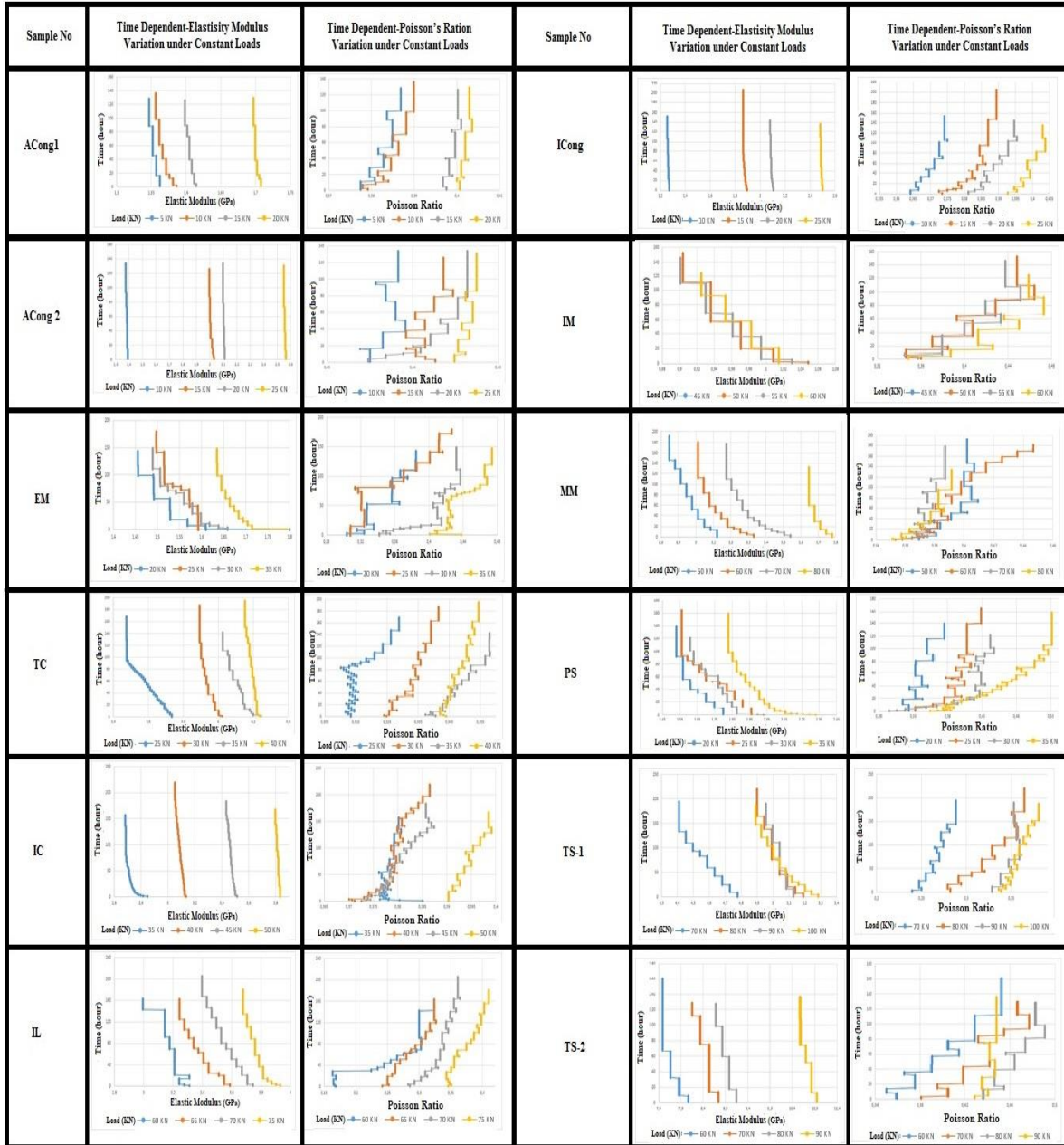


Fig. 5 Time-dependent variations in elastic modulus and Poisson's ratio under constant load

owing to the reason that the E_i values in the empirical equations are subject to change.

It can be clearly seen from Table 5 that E_i values will vary at different loads and that the values of E_{mass} in Table 6 will also change. Also, E_{mass} values calculated from empirical formulas developed by several researchers are given in Table 6. Obviously, there are differences between the E_{mass} values. Table 6 shows the E_{mass} value calculated using the E_i values obtained for different loads. E_{mass} values were calculated by replacing them with the formulas proposed by the same researchers. Thus, E_i changes in rock material under different loads allow the change of E_{mass} values. In this view, E_{mass} values, which represent rock masses that can be exposed to different loads, have become available.

2.2 Mathematical basis of the new approach

In this section, multivariable function $z=f(x,y)$ are

defined on R^3 . For functions of two variables the notation simply becomes $z=f(x,y)$ where the two independent variables are x and y , while z is the dependent variable. The surface $z=f(x,y)$ is considered to approximate over the rectangular region that is gridded by (x_i,y_j) on R^2 and $z_{ij}=f(x_i,y_j)$ data are given for the function of two variable at the distinct points in the rectangular region where x is load(kN) , y is time (h) and z is horizontal or vertical deformation.

With respect to graphs for given data, you can picture the partial derivative $\frac{\partial z}{\partial x}$ by slicing the graph of $z=f(x,y)$ with a plane representing a constant y -value and measuring the slope of the resulting curve along the cut and the partial derivative $\frac{\partial z}{\partial y}$ is differentiated with respect to y holding x constant.

Table 5 Variation of E_i from time-dependent tests on constant loads

		Variation of E_i from Time-Dependent Tests							
Maximum, Minimum and Average Value of E_i (MPa)	Sample	Afyon Conglomerate-1				Afyon Conglomerate-2			
	Load(kN)	5	10	15	20	10	15	20	25
	Max.	1570	1580	1620	1710	1400	2030	2100	2560
	Ave.	1550	1570	1610	1700	1390	2000	2090	2550
	Min.	1540	1560	1590	1690	1380	1990	2080	2540
	Sample	Eynez Marl				Tuncbilek Claystone			
	Load(kN)	20	25	30	35	25	30	35	40
	Max.	1610	1590	1660	1800	3720	4010	4200	4240
	Ave.	1530	1550	1580	1690	3570	3960	4130	4190
	Min.	1450	1500	1490	1630	3480	3900	4040	4160
Sample	Isiklar Marl				Isiklar Conglomerate				
Load(kN)	50	55	60		10	15	20	25	
Max.	1050	1030	1020	-	1280	1900	2120	2500	
Ave.	960	960	970	-	1250	1890	2100	2480	
Min.	900	900	920	-	1220	1880	2080	2460	
Sample	Isiklar Claystone				Isiklar Limestone				
Load(kN)	35	40	45	50	60	65	70	75	
Max.	2840	3140	3500	3390	3600	3600	3760	3920	
Ave.	2740	3100	3460	3180	3380	3380	3580	3800	
Min.	2680	3060	3420	2980	3240	3240	3400	3680	
Sample	Mesudiye Marl				Polyak Schist				
Load(kN)	50	60	70	80	20	25	30	35	
Max.	3120	3330	3540	3780	1800	1960	2030	2330	
Ave.	2990	3170	3360	3720	1670	1760	1820	2080	
Min.	2850	3010	3180	3650	1530	1550	1600	1830	
Sample	Topcam Sandstone-1				Topcam Sandstone-2				
Load(kN)	70	80	90	100	60	70	80	90	
Max.	4780	5200	5130	5280	8100	8800	9200	10900	
Ave.	4600	5100	5050	5090	7800	8500	8900	10700	
Min.	4410	4900	4960	4890	7500	8200	8700	10500	

Table 6 E_{mass} values obtained from current and from new integrated methodologies

		*Hoek and Diederichs (2006)				**Nicholson and Bieniawski (1990)				***Ramamurthy (2004)			
Sample		Afyon Conglomerate-1											
Static E_{mass} calculated from formula (MPa)		800				813				919			
	Load (kN)	5	10	15	20	5	10	15	20	5	10	15	20
E_{mass-v} (MPa)	Max	754	772	793	805	768	769	782	810	779	803	907	952
	Ave.	752	771	791	802	767	768	781	808	777	799	902	949
	Min	752	770	788	799	766	767	780	806	775	795	896	945
Sample		Afyon Conglomerate-2											
Static E_{mass} calculated from formula (MPa)		1200				1251				1727			
	Load (kN)	10	15	20	25	10	15	20	25	10	15	20	25
E_{mass-v} (MPa)	Max	1071	1124	1167	1197	1092	1115	1185	1242	1269	1525	1753	1940
	Ave.	1070	1122	1165	1195	1090	1112	1184	1241	1265	1517	1749	1936

Table 6 Continued

Sample		Afyon Conglomerate-2											
Static E_{mass} calculated from formula (MPa)		1200				1251				1727			
Load (kN)		10	15	20	25	10	15	20	25	10	15	20	25
Emass-v (MPa)	Min	1068	1119	1163	1191	1087	1111	1182	1239	1261	1509	1745	1932
	Ave.												
Sample		Eynez Marl											
Static E_{mass} calculated from formula (MPa)		1400				1478				1932			
Load (kN)		20	25	30	35	20	25	30	35	20	25	30	35
Emass-v (MPa)	Max	1347	1367	1398	1411	1386	1432	1465	2010	1462	1491	2086	2252
	Ave.	1340	1365	1396	1408	1382	1429	1463	2008	1459	1488	2085	2248
	Min	1333	1362	1394	1405	1377	1426	1460	2006	1456	1485	2084	2244
Sample		Tuncbilek Claystone											
Static E_{mass} calculated from formula (MPa)		2000				2059				2234			
Load (kN)		25	30	35	40	25	30	35	40	25	30	35	40
Emass-v (MPa)	Max	1951	1976	1992	2086	1987	2004	2059	2125	2000	2152	2238	2276
	Ave.	1948	1972	1987	2284	1983	2001	2053	2122	1998	2150	2234	2273
	Min	1945	1968	1982	2081	1979	1998	2047	2118	1996	2148	2229	2270
		*Hoek and Diederichs (2006)				**Nicholson and Bieniawski (1990)				***Ramamurthy (2004)			
Sample		Isiklar Marl											
Static E_{mass} calculated from formula (MPa)		619				626				684			
Load (kN)		50	55	60		50	55	60		50	55	60	
Emass-v (MPa)	Max	596	612	623		605	623	636		619	665	714	
	Ave.	594	610	619		602	615	632		615	659	712	
	Min	592	607	615		599	607	627		611	654	709	
Sample		Isiklar Conglomerate											
Static E_{mass} calculated from formula (MPa)		3360				3378				3941			
Load (kN)		10	15	20	25	10	15	20	25	10	15	20	25
Emass-v (MPa)	Max	2710	2788	3326	3354	3071	3143	3215	3367	3371	3679	3912	4147
	Ave.	2700	2777	3323	3345	3025	3113	3203	3363	3367	3634	3901	4108
	Min	2689	2765	3319	3336	2978	3083	3191	3358	3362	3589	3890	4069
Sample		Isiklar Claystone											
Static E_{mass} calculated from formula (MPa)		2300				2525				2710			
Load (kN)		35	40	45	50	35	40	45	50	35	40	45	50
Emass-v (MPa)	Max	2260	2287	2320	2310	2298	2336	2354	2583	2378	2524	2698	2755
	Ave.	2251	2284	2317	2291	2293	2334	2351	2579	2373	2511	2689	2751
	Min	2245	2280	2313	2273	2287	2331	2348	2574	2367	2498	2679	2746
Sample		Isiklar Limestone											
Static E_{mass} calculated from formula (MPa)		1800				1896				1939			
Load (kN)		60	65	70	75	60	65	70	75	60	65	70	75
Emass-v (MPa)	Max	1615	1626	1742	1840	1743	1850	1915	1960	1909	1939	1994	2079
	Ave.	1585	1615	1732	1835	1735	1836	1889	1947	1898	1931	1984	2056
	Min	1554	1604	1721	1829	1727	1821	1862	1933	1886	1923	1973	2032
		*Hoek and Diederichs (2006)				**Nicholson and Bieniawski (1990)				***Ramamurthy (2004)			

Table 6 Continued

Sample		Mesudiye Marl											
Static E_{mass} calculated from formula (MPa)		740				785				959			
Load (kN)		50	60	70	80	50	60	70	80	50	60	70	80
Emass-v (MPa)	Max	665	697	713	742	708	752	793	836	761	833	927	1066
	Ave.	662	694	710	739	702	745	789	827	753	829	920	1063
	Min	658	691	706	735	696	737	784	817	745	824	912	1059
Sample		Polyak Schist											
Static E_{mass} calculated from formula (MPa)		1200				1268				1910			
Load (kN)		20	25	30	35	20	25	30	35	20	25	30	35
Emass-v (MPa)	Max	1141	1172	1207	1224	1177	1214	1268	1313	1841	1916	1948	1989
	Ave.	1137	1169	1203	1219	1169	1208	1262	1307	1780	1822	1850	1952
	Min	1133	1165	1198	1213	1161	1201	1256	1300	1715	1724	1748	1915
Sample		Topcam Sandstone-1											
Static E_{mass} calculated from formula (MPa)		1440				1532				2881			
Load (kN)		70	80	90	100	70	80	90	100	70	80	90	100
Emass-v (MPa)	Max	1188	1284	1368	1402	1503	1553	1628	1682	2700	2938	2898	2983
	Ave.	1146	1250	1349	1459	1483	1520	1603	1662	2599	2881	2853	2873
	Min	1104	1215	1329	1408	1462	1486	1578	1643	2491	2768	2802	2763
Sample		Topcam Sandstone-2											
Static E_{mass} calculated from formula (MPa)		4800				4865				6074			
Load (kN)		60	70	80	90	60	70	80	90	60	70	80	90
Emass-v (MPa)	Max	2921	3174	3318	3531	3879	4215	4406	4715	5464	5936	6206	6523
	Ave.	2813	3066	3210	3509	3736	4071	4287	4683	5262	5747	6004	6500
	Min	2705	2957	3138	3487	3592	3927	4167	4651	5059	5532	5869	6477

*Hoek and Diederichs (2006): $E_{mass} = E_i (0.02 + \frac{1+D/2}{1+e^{(60+15D-GSI)/11}})$

**Nicholson and Bieniawski (1990): $E_{mass} = \frac{E_i}{100} (0.0028RMR^2 + 0.9\exp(\frac{RMR}{22.82}))$

***Ramamurthy (2004): $E_{mass} = E_i e^{-0.0035 [250 (1-0.3\log Q)]}$

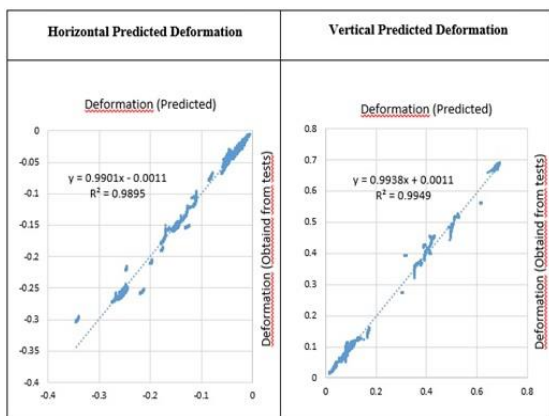


Fig. 6 Performance of new formula to predict horizontal and vertical deformation

When the variable time y_j of interest for given data are held fixed during the differentiation, the partial derivative $\frac{\partial z}{\partial x}$

$$\lim_{h \rightarrow 0} \frac{f(x_i + h, y_j) - f(x_i, y_j)}{h} = \frac{\partial z_{ij}}{\partial x_i} \cong b \frac{z_{ij}}{x_i} \quad (1)$$

is numerically computed. The same calculation of partial derivative $\frac{\partial z}{\partial y}$ with respect to variable load y_j is calculated as

$$\lim_{h \rightarrow 0} \frac{f(x_i, y_j + h) - f(x_i, y_j)}{h} = \frac{\partial z_{ij}}{\partial x_i} \cong c \frac{z_{ij}}{y_j} \quad (2)$$

where coefficients of b and c are evaluated numerically from the given data with relationship above derivatives.

In general, the total differential dz of the function $f(x,y)$ is defined as

$$dz = \frac{\partial f}{\partial x} dx + \frac{\partial f}{\partial y} dy \quad (3)$$

Let us suppose that

$$\frac{\partial f}{\partial x} = \frac{\partial z}{\partial x} = b \frac{z}{x} \quad \text{and} \quad \frac{\partial f}{\partial y} = \frac{\partial z}{\partial y} = c \frac{z}{y} \quad (4)$$

This differential is

$$dz = b \frac{z}{x} dx + c \frac{z}{y} dy \quad (5)$$

and the general solution is obtained as

$$\frac{dz}{z} = b \frac{dx}{x} + c \frac{dy}{y} \quad (6)$$

$$\int \frac{dz}{z} = b \int \frac{dx}{x} + c \int \frac{dy}{y} \quad (7)$$

$$\text{Ln}z = b \text{Ln}x + c \text{Ln}y + k \quad (8)$$

$$z = e^{b \text{Ln}x + c \text{Ln}y + k} = e^k e^{\text{Ln}x^b} e^{\text{Ln}y^c} \quad (9)$$

Using numerical approach for given data, the approximation function can be formulated as

$$z = ax^b y^c \quad (10)$$

The solution of the differential where $a=e^k$ and k is integral constant.

Data analysis and mathematical studies showed that new equations that can describe the deformation characteristics of rock masses can be developed. Hence, Eq. (11) was developed to represent time-dependent and load-dependent deformation behaviour of rock masses. Predicted performance of this equation was determined as $R^2=0.9895$ for horizontal deformation and $R^2=0.9949$ for vertical deformation (Fig. 6).

$$\varepsilon = a.F^b.t^c.(\sigma_{ci})^d \quad (11)$$

where; a , b , c , and d are constants, ε is deformation (vertical and horizontal), F is load (kN), t is time (h) and σ_{ci} is uniaxial compressive strength of rock material. The coefficients a , b , and c are derived from time dependent experiments in servo-controlled press under various constant loads. A sub-routine has been developed to integrate the new formula into numerical modeling software.

In time-dependent numerical analysis, the loads to which the rock is subjected to vary with time. This equation has the ability to represent the rocks with different characteristics. The equation also can represent time-dependent behavior of rock for the load to which the rock is subjected during the numerical modeling phases.

2.3 Numerical modeling sub-routine

The software development environment "Intel Parallel Studio XE 2017 Intel® Visual Fortran Compiler" (2017) was used for the sub-routine developed in the study. Geany (2018) is used as the code editor. A user defined - DLL

(Dynamic Link Library) was created and imported to the Plaxis 3D (2018) software. In the subroutine, the results obtained from the experimental results were taken as parameters and 3D rock modeling was performed according to time variation. The subroutine developed performs its operation with following algorithm (Fig. 7).

According to time deformation algorithm, parameters are taken first and realistic calculation process is started. In realistic calculation steps; stress value is calculated. The value resulting from the stress calculation is checked to find the near load value and the values of E_i , ν , E_{mass} are calculated using these obtained values. To find the time-dependent deformation, the bulk modulus (K) and shear modulus (G) are obtained using the calculated E_{mass} value. Following these steps, horizontal and vertical deformations are calculated and assigned to the relevant parameter on the model. The same calculation process is continued until reaching the time.

2.4 Field and numerical modelling studies

An equation was developed in which the deformation behaviors of the rocks are represented by time at different constant loads from the laboratory and software studies carried out during the research. This formula is integrated into the numerical modeling software. 12 different tunnel and mine colliary faces have been investigated in 7 different projects using this equation. Each project has separate excavation and support phases. Convergence measurement stations were set up to measure the vertical deformations at the point where the excavation was performed and the measurements were conducted for 25 days. In field measurements, it was determined that the deformations recorded in the measurement stations stopped before 25 days. Excavation-support practices, which have always been carried out in a field study, have been integrated into individual models. The comparison of the vertical deformation measurements carried out in the field and the vertical deformation values obtained from the numerical modeling are given in Figure 8.

There are significant similarities between field measurements and the results obtained from numerical modeling, as seen in Figure 8. In this case, precise results can be obtained with the new equations developed considering time dependency and load dependency. Mohr-Coulomb failure criterion is used in numerical models.

3. Results and discussions

Numerical modeling techniques are extensively used as the tool to perform stress-strain analysis in which changing load and the amount of deformation in rock mass are analysed due to applied load. These tools can be successfully used in many engineering projects.

In order to determine E_i , which is one of the most important parameters used in the design of rock / soil structures, deformation experiments were carried out as time-dependent and in different constant loads in the laboratory. It was determined that the deformations in the samples became stable after about 200 hours during these

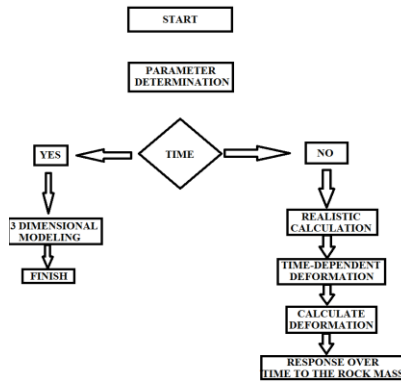


Fig. 7 Numerical modeling sub-routine algorithm

example, experiments were carried out on the EM sample

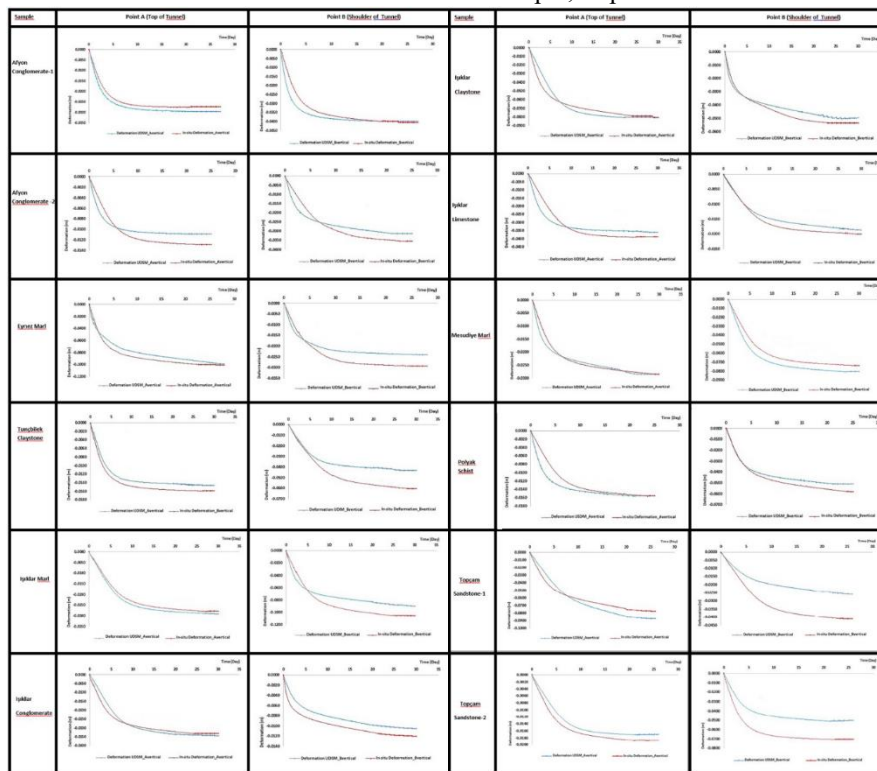


Fig. 8 Comparison of vertical deformation obtained from field measurements and numerical modeling

experiments. When the test results are examined, it is determined that the e_i value under constant load increases over time. The main reason for this is that the empty volumes in the sample and the possible minor discontinuities in the final stage of the experiments are closed. After this stage, no deformation changes were observed in any of the samples. When the test results were examined, it is seen that the amount of load applied to the samples increased and the E_i value increased

Fig. 5 shows the variations in E_i and v of the rocks from time-dependent deformations under constant loads applied on different rock types sampled from different regions. Important result obtained in some experiments can be expressed as that E_i curves clustered under changing loads. However, just one part of the curve can be distinguished from the others. At this stage, E_i values can be much different from the previous behavior under any load. For

with 4 different loads. The curves appear to be clustered at 3 (20, 25 and 30 kN) of the experiments and the experimental curve under 35 kN load was separately located in other experimental curves. At the same time, there is also a difference in the trends of the curves. E_i was reduced from 1.60 GPa to 1.45 GPa after 143 hours of the outset of the experiment when a load of 20 kN was applied on EM sample. Reduction rate in 143 hours was about 9,38%. Then, after 177 hours of the outset of the experiment, E_i was reduced from 1.59 GPa to 1.49 GPa when a load of 25 kN was applied. The reduction rate in E_i after 177 hours of the outset of the experiment was obtained to be 6,29%. In an experiment with an applied load of 30 kN, E_i decreased from 1.65 GPa to 1.48 GPa in 147 hours of the outset of the experiment with a reduction rate of 10,31%. In another experiment with an applied load of 35 kN, E_i was reduced

from 1.71 GPa to 1.63 GPa after 147 hours with a reduction rate of 4.68%. Laboratory works are conducted to understand the deformation behavior of rock materials as a function of time and load dependency.

Mathematical studies were performed by analyzing the obtained data. With the data analysis performed, a formula has been produced which shows the time and load related deformation behaviors of rock/soil samples. The uniaxial compressive strength of the rock material is also integrated into the formulation as a parameter so that the formula can represent more rock materials. With the newly produced formula, it is possible to calculate the E_{mass} value that the rock mass can have as time and loads dependent. As stated in the text, the correlation coefficients of this equation for rock material were found as $R^2 = 0.9949$ and $R^2 = 0.9895$ for vertical and horizontal deformations, respectively. Table 3 shows the E_i values obtained as a result of the deformation tests performed by the classical method. Table 4 shows the E_i values obtained from time-dependent deformation experiments under different constant loads. Considering the E_i values in both tables significant differences are observed. For example, the E_i value obtained from the classical deformation experiment in the Afyon Konglomera sample is 1180 MPa, while the E_i minimum 1540 MPa and maximum 1710 MPa can be realized as a result of time-dependent deformation experiments under different constant loads. According to these results, the E_i value obtained from the experiments carried out under time and different constant loads is 30.5-44.91% higher than the E_i values obtained from the classical method experiment. In contrast to this, the E_i value obtained by the classical deformation test in the Topcam Sandstone-2 sample was 12020 MPa, while the E_i values could be minimum 7500 MPa and maximum 10900 MPa as a result of the deformation experiments performed under different constant loads depending on time. In this case, the E_i values obtained by the new method can be as small as 9.32-37.60% by the conventional method. In these two examples, the E_i value obtained by the classical method is more or less in the E_i values obtained from the deformation experiment under time-dependent constant loads. The more complex one is the Polyak schist sample. The E_i value obtained as a result of the classical deformation test performed on this sample is 2090 MPa. The minimum E_i value obtained from the deformation experiments carried out under time and constant loads on this sample is 1530 MPa maximum value 2330 MPa. In this case, the E_i values used in the new method can be 24.79% or 11.48% higher than the E_i value obtained by the conventional method. The important thing in the design phase is to calculate the load that the rock mass will be exposed to, which is not an easy thing. Moreover, it is important to remember that the loads have changed or repeated continuously during the excavation phases. For the E_{mass} values used in the design, it would be correct to make an evaluation based on the discussion of the values given in Tables 4 and 5. Table 6 shows the E_{mass} values calculated by empirical equations proposed by different researchers. Static E_{mass} values are the values in which the E_i value in the formula is obtained by the classical deformation test. E_{mass-v} values are obtained by using the E_i values obtained by time dependent deformation tests under different constant loads in the related formula. In this case, the static e_{mass} value calculated for Afyon

Konglomera-1 rock mass is 800 MPa for the formula of Hoek and Diederich (2006), 813 MPa for the formula of Nicholson and Bieniawski (1990) and 919 MPa for the Ramamurty (2004) formula. According to Hoek and Diederich (2006) formula, 752-805 MPa, 766-810 MPa for the formula of Nicholson and Bieniawski (1990) and 775-952 for Ramamurty (2004) formula under E_i values obtained from deformation experiments under time and constant loads. It can take MPa values. In the case of the Hoek and Diederich (2006) formula, the E_{mass} value obtained in the conventional method may be approximately 6% lower than the value obtained by the new method or 1% higher. This difference may be more or less in other examples. This is particularly important for the design of rock masses, which score close to the boundary zones in rock mass classification systems during preliminary design.

In laboratory deformation experiments, it has been confirmed that the rocks have different E_i and poisson ratio under different applied loads. E_{mass} values, which can be predicted by empirical equations, will differ as E_i value in empirical equations changes. In this case, different E_{mass} values are obtained for different applied loads. Different E_{mass} values allow the rock mass to exhibit different deformation behaviors under different loads in time.

A sub-routine, which contains new formula and algorithm, was developed. This sub-routine is integrated into the numerical modeling software. In this case, a new integrated method was created in which the rock/soil structure exposed to different loads could receive different E_{mass} values with different E_i values. This integrated method, depending on time and loads, may represent different rock/soil mass deformation behavior under different loads. Numerical modeling results with newly developed integrated time and load dependent deformation equation and field measurement results are illustrated in Fig. 8. When the results are evaluated, it can be seen that numerical results will be very close to that obtained in the field.

4. Conclusions

Numerical modeling techniques are very extensively used in rock mechanics in recent years. Parameters related to rock mass are input in numerical models especially in the analysis of stress and strain. The success of numerical analyses will depend on how accurately those parameters will be chosen to truly represent the rock mass. One of the purposes of the numerical modeling is to analyse step by step the engineering operations carried out in the field. One of factors for success of the numerical model is related to the accuracy in which the model is integrated into the application. Rock engineering experts know that; when an excavation is started in a rock mass, the primary stresses will re-distribute. Hence, primary stress state will be transformed into secondary state of stress and even tertiary stress depending on the rock mass in certain cases. Briefly, the state of stress changes with the existence of an excavation. This change may occur over the time. The point at which the excavation is carried out is influenced by variable loads for a certain period of time. This time depends on the speed of advance of the excavation, and the

loads are stabilized as they are often about 2-3 times the diameter of the opening. Rock mass is constantly exposed to different loads up to this stage. In this case, instead of using a single and constant E_{mass} and ν values in numerical models, using different E_{mass} and ν values under various loads will yield more precise results.

The main purpose of this research is to integrate this time-dependent properties of rock masses with different elastic behaviors under different loads into numerical analyses. The results have shown that application of new method will provide more precise results in the numerical models. This will allow for the design of safer rock / soil structures.

Acknowledgments

This research was carried out under the project numbered 114M566 supported by TUBITAK. The authors would like to thank TUBITAK for their support.

References

- Aksoy, C.O., Uyar, G.G., Posluk, E., Ogul, K., Topal, I. and Kucuk, K. (2016), "Non-deformable support system application at tunnel-34 of Ankara-Istanbul high speed railway project", *Struct. Eng. Mech.*, **58**(5), 869-886. <https://doi.org/10.12989/sem.2016.58.5.869>.
- Aksoy, C.O., Geniş, M., Aldas, G.G., Özacar, V., Ozer, S.C. and Yılmaz, Ö. (2012), "A comparative study of the determination of rock mass E_{mass} by using different empirical approaches", *Eng. Geol.*, **131-132**, 19-28.
- Andersson, J.A., Munier, R., Strom, A., Soderback, B., Almen, K.E. and Olsson, L. (2004), "When is there sufficient information from the site investigations?", SKBReportR-04-23, Stockholm, Sweden, www.skb.se.
- Azarafza, M., Akgün, H. and Asghari-Kaljahi, E. (2017), "Assessment of rock slope stability by slope mass rating (SMR): A case study for the gas flare site in Assalouyeh, South of Iran", *Geomech. Eng.*, **13**(4), 571-584. <https://doi.org/10.12989/gae.2017.13.4.571>.
- Barla, G. (1995), "Tunneling under squeezing rock conditions", Project no: 9708328160/1998, Politecnico di Torino, Turin, Italy.
- Barton, N. (2002), "Some new Q value correlations to assist in site characterization and tunnel design", *Int. J. Rock Mech. Min. Sci.*, **39**, 185-216. [https://doi.org/10.1016/S1365-1609\(02\)00011-4](https://doi.org/10.1016/S1365-1609(02)00011-4).
- Bieniawski, Z.T. (1973), "Engineering classification of jointed rock masses", *Trans. S. Afr. Inst. Civ. Eng.*, **15**(12), 335-344.
- Edelbro, C., Sjöberg, J. and Nordlund, E. (2006), "A quantitative comparison of strength criteria for hard rock masses", *Tunn. Undergr. Sp. Technol.*, **22**(1), 57-68. <https://doi.org/10.1016/j.tust.2006.02.003>.
- Feng, X.T. and An, H. (2004), "Hybrid intelligent method optimization of a soft rock replacement scheme for a large cavern excavated in alternate hard and soft rock strata", *Int. J. Rock Mech. Min. Sci.*, **41**(4), 655-667. <https://doi.org/10.1016/j.ijrmms.2004.01.005>.
- Feng, X.T. and Hudson, J.A. (2004), "The ways ahead for rock engineering design methodologies", *Int. J. Rock Mech. Min. Sci.*, **41**(2), 255-273. [https://doi.org/10.1016/S1365-1609\(03\)00112-6](https://doi.org/10.1016/S1365-1609(03)00112-6).
- Feng, X.T. and Hudson, J.A. (2010), "Specifying the information required for rock mechanics modelling and rock engineering design", *Int. J. Rock Mech. Min. Sci.*, **47**(2), 179-194. <https://doi.org/10.1016/j.ijrmms.2009.12.009>.
- Geany-The Flyweight IDE (2018), Geany Code Editor, Oberhausen, Germany. <https://www.geany.org/download/releases/>
- Gokceoglu, C., Sonmez, H. and Kayabasi, A. (2003), "Predicting the deformation moduli of rock masses", *Int. J. Rock Mech. Min. Sci.*, **40**(5), 701-710. [https://doi.org/10.1016/S1365-1609\(03\)00062-5](https://doi.org/10.1016/S1365-1609(03)00062-5).
- Gu, J. (2015), "Some practical considerations in designing underground station structures for seismic loads", *Struct. Eng. Mech.*, **54**(3), 491-500. <https://doi.org/10.12989/sem.2015.54.3.491>.
- Hoek, E. and Brown, E.T. (1997), "Practical estimates of rock mass strength", *Int. J. Rock Mech. Min. Sci.*, **34**(8), 1165-1186. [https://doi.org/10.1016/S1365-1609\(97\)80069-X](https://doi.org/10.1016/S1365-1609(97)80069-X).
- Hoek, E. and Diederichs, M.S. (2006), "Empirical estimation of rock mass modulus", *Int. J. Rock Mech. Min. Sci.*, **43**, 203-215. <https://doi.org/10.1016/j.ijrmms.2005.06.005>.
- Hudson, J.A. and Feng, X.T. (2007), "Updated flowcharts for rock mechanics modelling and rock engineering design", *Int. J. Rock Mech. Min. Sci.*, **44**(2), 174-195. <https://doi.org/10.1016/j.ijrmms.2006.06.001>.
- Intel Parallel Studio XE (2017), Intel Parallel Studio XE for Windows Visual Fortran Compiler, U.S.A. <https://software.intel.com/en-us/parallel-studio-xe/choose-download/free-trial-cluster-windows-c-fortran>.
- Jing, L. and Hudson, J.A. (2002), "Numerical methods in rock mechanics", *Int. J. Rock Mech. Min. Sci.*, **39**(4), 409-427. [https://doi.org/10.1016/S1365-1609\(02\)00065-5](https://doi.org/10.1016/S1365-1609(02)00065-5).
- Kayabasi A. Gokceoglu, C. and Ercanoglu, M. (2003), "Estimating the deformation modulus of rock masses: A comparative study", *Int. J. Rock Mech. Min. Sci.*, **40**, 55-63. [https://doi.org/10.1016/S1365-1609\(02\)00112-0](https://doi.org/10.1016/S1365-1609(02)00112-0).
- Mazzoccola, D.F., Millar, D.L. and Hudson, J.A. (1997), "Information, uncertainty and decision making in site investigation for rock engineering", *Geotech. Geol. Eng.*, **15**(2), 145-180. <https://doi.org/10.1007/BF00880754>.
- Mitri, H.S., Edrissi, R. and Henning, J. (1994), "Finite element modelling of cable-bolted stopes in hardrock ground mines", *Proceedings of the SME Annual Meeting*, Albuquerque, New Mexico, U.S.A., February.
- Nicholson, G.A. and Bieniawski, Z.T. (1990), "A nonlinear deformation modulus based on rock mass classification", *Int. J. Min. Geol. Eng.*, **8**(3), 181-202. <https://doi.org/10.1007/BF01554041>.
- Palchik, V. (2018), "Applicability of exponential stress-strain models for carbonate rocks", *Geomech. Eng.*, **15**(3), 919-925. <https://doi.org/10.12989/gae.2018.15.3.919>.
- Palmstrom, A. and Singh, R. (2001), "The deformation modulus of rock masses-comparisons between in situ tests and indirect estimates", *Tunn. Undergr. Sp. Technol.*, **16**(2), 115-131. [https://doi.org/10.1016/S0886-7798\(01\)00038-4](https://doi.org/10.1016/S0886-7798(01)00038-4).
- Palmstrom, A. and Stille, H. (2007), "Ground behaviour and rock engineering tools for underground excavations", *Tunn. Undergr. Sp. Technol.*, **22**(4), 363-376. <https://doi.org/10.1016/j.tust.2006.03.006>.
- Palmström, A. (1995), "RMi-a rock mass characterization system for rock engineering purposes", Ph.D. Thesis, University of Oslo, Oslo, Norway.
- Palmström, A. (1996), "Characterizing rock masses by the RMi for use in practical rock engineering, Part 2: Some practical applications of the rock mass index (RMi)", *Tunn. Undergr. Sp. Technol.*, **11**(3), 287-303. [https://doi.org/10.1016/0886-7798\(96\)00028-4](https://doi.org/10.1016/0886-7798(96)00028-4).
- Plaxis (2018), *Plaxis Geotechnical Engineering Software*,

Tutorial.

- Read, S.A.L., Richards, L.R. and Perrin, N.D. (1999), "Applicability of the Hoek-Brown failure criterion to New Zealand greywacke rocks", *Proceedings of the 9th International Congress on Rock Mechanics*, Paris, France, August.
- Rooh, A., Nejati, H.R. and Goshtasbi, K. (2018), "A new formulation for calculation of longitudinal displacement profile (LDP) on the basis of rock mass quality", *Geomech. Eng.*, **16**(5), 539-545. <https://doi.org/10.12989/gae.2017.13.4.571>.
- Sefarim, J.L. and Pereira, J.P. (1983), "Consideration of the geomechanics classification of Bieniawski", *Proceedings of the International Symposium on Engineering Geology and Underground Construction*, Lisbon, Portugal.
- Sonmez, H., Gokceoglu, C. and Ulusay, R. (2004), "Indirect determination of the modulus of deformation of rock masses based on the GSI system", *Int. J. Rock Mech. Min. Sci.*, **41**(5), 849-857.
- Sonmez, H., Gokceoglu, C., Nefeslioglu, H.A. and Kayabasi, A. (2006), "Estimation of rock modulus: for intact rocks with an artificial neural network and for rock masses with a new empirical equation", *Int. J. Rock Mech. Min. Sci.*, **43**(2), 224-235. <https://doi.org/10.1016/j.ijrmms.2005.06.007>.
- Taravati, H. and Ardakani, A. (2018), "The numerical study of seismic behavior of gravity retaining wall built near rock face", *Earthq. Struct.*, **14**(2), 179-186. <https://doi.org/10.12989/eas.2018.14.2.179>.
- Zhang, Y., Ding, X., Huang, S., Qin, Y., Li, P. and Li, Y. (2018), "Field measurement and numerical simulation of excavation damaged zone in a 2000 m-deep cavern", *Geomech. Eng.*, **16**(4), 339-413. <https://doi.org/10.12989/gae.2018.16.4.399>.